

# Phase behavior of rod-like virus and polymer mixtures

BY ZVONIMIR DOGIC AND SETH FRADEN

*The Complex Fluid Group, Martin Fisher School of Physics,  
Brandeis University, Waltham Massachusetts 02454*

We have prepared a homologous series of filamentous viruses with varying contour length using molecular cloning techniques. These viruses are monodisperse enough to form a stable smectic phase. Two systems are studied. The first system consists of viruses to which polymers are covalently attached to the virus surface. Through studies of the isotropic - cholesteric phase transition we demonstrate that covalently attached polymers alter the effective diameter of the virus. Additionally, we have produced mixtures of viruses whose ratio of effective diameters varies by a factor of five. The second system is composed of mixtures of rod-like viruses and non-absorbing polymers. With this system we study the kinetics of the isotropic - smectic phase transition and describe observations of a number of novel metastable structures of unexpected complexity.

**Keywords: Depletion Interaction; Isotropic-Smectic Phase Transition;  
Hard-rod Fluids**

## 1. Introduction

Observation of the nematic phase in aqueous suspensions of rod-like TMV (tobacco mosaic virus) served as an inspiration for Onsager to write his seminal paper on the isotropic-nematic (I-N) phase transition in hard rods (Onsager 1949). Ever since then biopolymers (DNA, TMV, *fd*) have served as an important model system of hard rods and have often been used to test the Onsager theory and its various extensions (Meyer 1990; Fraden 1995; Livolant 1991). In section 2 of this paper we briefly outline the advantages of using the semi-flexible rod-like *fd* or closely related M13 virus as a model system of hard rods. We demonstrate that using standard procedures of molecular cloning it is possible to construct genetically modified viruses with widely varying contour length. These viruses are monodisperse enough to form a stable smectic phase. In section 3 we outline the synthesis of a *fd*-polymer complex and show that polymers covalently attached to the virus effectively increase the diameter of the rods. By changing the ionic strength it is possible to observe the crossover from the regime where the rods are electrostatically stabilized to where they are stabilized by repulsion between attached polymers. This synthesis is a convenient way to alter the diameter of the rod and enables us to study bi-disperse rod suspensions with different diameters. In section 4 we outline the phase behavior of mixtures *fd* virus with non-absorbing polymer. In particular we focus on the isotropic-smectic phase transition and describe a number of different pathways

in which the smectic phase nucleates and grows out of an isotropic suspension of viruses.

## 2. *fd* virus as a versatile model system of hard rods

TMV and *fd* viruses form, in order of increasing concentration of rods, a stable isotropic, nematic or cholesteric, and smectic phase (Wen *et al.*; Dogic & Fraden 1997; Dogic & Fraden 2000). These two experimental colloidal systems are the only ones that follow the sequence of liquid crystalline phase transitions that have been predicted by the theory and computer simulations of hard rods (Bolhuis & Frenkel 1997; Vroege & Lekkerkerker 1992). Paucity of systems exhibiting smectic phases is presumably due to polydispersity, which is inherently present in all other polymeric and colloidal experimental systems due to the fact that they are chemically synthesized. In contrast to chemical synthesis, Nature uses DNA technology to produce viruses that are identical to each other, which results in highly monodisperse viruses. This high monodispersity of virus suspensions is the property that makes them an appealing system to experimentally study the phase behavior of hard rods.

However, there are several important disadvantages that viruses have compared to synthetic rod-like polymers. Firstly, although rod-like viruses have very well defined lengths and diameters studies of how the phase behavior depends on the length to diameter ratio are non-existent for virus suspensions. Secondly, the viruses are charged stabilized and therefore their interactions are not truly hard rod interactions, but in addition to steric repulsion, have a long range soft repulsion. It is important to note that because of the small diameter of the virus the range of this electrostatic repulsion is always comparable to the hard core diameter for the range of ionic strengths for which the stability of the virus against aggregation is not compromised. Also, because of its protein structure it is impossible to dissolve the virus in apolar or weakly polar solvents and preserve the colloidal stability of the virus. It has also been observed that the virus aggregates in an ionic solution of multivalent cations. In this section we show that using standard biological methods it is possible to alter the contour length of the virus while preserving the monodispersity of the virus. In the subsequent section we show that by covalently attaching polymer onto the virus surface we can alter the effective diameter of the virus, and we have achieved stability of the virus even in the presence of multivalent cations. It is our hope that the introduction of these methods will make the viruses a more appealing model system with which to study phase behavior of rods.

We note that M13 virus with length (L) diameter (D) ( $L/D \approx 130$ ) and construct M13- $T_n$ 3-15 ( $L/D \approx 240$ ) were used in the studies of the concentration dependence of rotational diffusion almost 20 years ago (Maguire *et al.*) 1980. However, this potentially powerful method was never pursued in subsequent studies. M13 virus is genetically almost identical to *fd* and has the same contour length with coat proteins differing by only a single amino acid; negatively charged aspartate in *fd* (asp<sub>12</sub>) corresponding to neutral asparagine in M13 (asn<sub>12</sub>) (Bhattacharjee *et al* 1992). This change in a single amino-acid alters the surface charge by about 30 percent and M13 can easily be distinguished from *fd* by gel electrophoresis. All our clones have their origin in M13 virus, which also means that they have lower surface charge than *fd* wild type (*wt*) system.

Since all available data indicates that the length of the virus is linearly proportional to the length of the DNA contained in the virus, the virus length can be extended by simply introducing foreign DNA into M13 wt DNA using restriction endonucleases (Herrmann *et al.* 1980). However, during large scale preparation we found that the mutant virus would often quickly revert to its wild type form by deleting the foreign DNA. Another disadvantage of this method is that it is impossible to construct clones that are shorter than M13 wt. Because of these reasons we used a well documented phagemid method to prepare our rod-like viruses with variable contour length (Maniatis *et al.* 1989). This method allows us to grow clones that are both longer and shorter than M13 wt. The disadvantage of the phagemid method is that the helper phage M13KO7 (a virus with contour length  $1.2 \mu\text{m}$ ) is always present in the final suspension. The volume fraction of the helper phage depends on the bacterial host and can vary from 20% (E. Coli. JM 101) to 5% (E. Coli. XL-1 Blue). Typically, 0.5 - 1 gram of purified virus can be obtained in one to two weeks of work. We found that it is possible to separate the clones from the  $1.2 \mu\text{m}$  long helper phage by adjusting the concentration of the bi-disperse, purified virus suspension such that it is in I-N coexistence. There is a strong fractionation effect at the I-N transition for bidisperse rods, with large rods almost entirely dispersed in nematic phase as is predicted by the theory (Lekkerkerker *et al.* 1984, Sato & Teramoto 1994). Therefore, by keeping only the portion of the suspension in the isotropic phase we can obtain rods with higher monodispersity.

All of the viruses grown using the phagemid method are monodisperse enough to form stable smectic phases as is illustrated in Fig. 1. We note that the measured spacing of the smectic phase ( $\lambda$ ) is almost identical to the contour length ( $L$ ) for all the mutants studied. The qualitative trend that flexibility decreases the smectic layering has been predicted theoretically and observed experimentally (Dogic & Fraden 1997, Polson & Frenkel 1997, van der Schoot 1996, Tkachenko 1996). Unfortunately, the theories are not accurate enough to be able to quantitatively predict dependence of smectic spacing on the flexibility of the rod. We expect that the persistence length ( $P \sim 2.2 \mu\text{m}$ ) of all our clones is the same, because all clones have the same structure and only vary in length. Since the contour length varies, so to does the ratio of contour to persistence length  $L/P$ . Thus we expected that the shorter rods ( $L = 0.4 \mu\text{m}$ ) would be relatively stiffer than the longer ones ( $L = 1.4 \mu\text{m}$ ) and consequently predicted that the layer spacing would increase for shorter rods. This was not the case as we observed that for all lengths the ratio  $\lambda/L \sim 1$ .

We also find out that *fd wt* (Fig 1c) consistently forms a smectic phase at a lower concentration than M13 constructs. This is perhaps explained by the difference in surface charge between M13 and *fd* and the breakdown of the concept of effective diameter at high concentrations. The *fd wt* is more charged than M13 and therefore the highly concentrated aligned rods in nematic phase repel each other more strongly, which results in a higher effective concentration and thus the nematic-smectic phase transition occurs at a lower number density of rods. Note that at low concentrations changing the surface charge by 30% has negligible effect on the effective diameter and the phase behavior of the isotropic - nematic transition (Fig. 1 in Tang and Fraden (1995)).

With the availability of rods with different contour length we are able to experimentally explore a number of important issues pertaining to the phase behavior of hard rods. For pure rods we can address the question of how flexible can a particle

be and still form a smectic phase. Another important question is the relative stability of columnar and smectic phase as a function of rod bidispersity or polydispersity (Bates & Frenkel 1998, Bohle *et al.* 1996, Stroobants 1992, van Roij & Mulder 1996, Cui & Chen 1994). For mixtures whose lengths are different enough there is also a prediction of microseparated smectic phase (Koda & Kimura 1994). So far there are no experimental studies on these subjects, but with our system we can prepare artificially polydisperse and bidisperse suspensions to explore these issues.

### 3. *fd* virus with covalently attached polymer

Besides preparing viruses with varying contour length we are also able to alter the effective diameter of the virus by coating it with the polymer. The amino terminal group of each coat protein of *fd* and M13 virus is exposed to the solution. Through this chemical site we are able to covalently attach water soluble polymer Poly(ethylene glycol) (PEG) to the surface of the virus. End functionalized PEG molecules that readily attaches to amino groups were obtained from Shearwater polymers. The chemical reaction was carried out in 100 mM phosphate buffer at pH 7.5 for 30 minutes and the virus concentration was kept at 1 mg/ml. For SSA-PEG-5000 the concentration of PEG was kept the same as the concentration of the virus in the reaction vessel while for SPA-PEG-20000 the concentration was four-fold the virus concentration. The reaction product (*fd*-PEG) was separated from unreacted PEG polymer by repeated centrifugation at 200,000 g. The pellet contained the nematic phase of the *fd*-PEG complex. We diluted a few samples to the concentration of the isotropic-nematic phase co-existence, and after an exceedingly long time (up to few months), we observed macroscopic phase separation. The measured width of the co-existing concentrations did not differ from the measured width in *fd wt*, which is about 10% (Tang & Fraden 1995). This is an indication that the absorbed polymer does not significantly alter the flexibility of the rod-like particles. We infer this from the well established fact that the width of the I-N coexistence is very sensitive to the flexibility of the rod (Chen 1993). If we had observed widening of the I-N coexistence it would have been an indication that polymer effectively increases rigidity of the rod. Because of the extremely long time required for complete phase separation, in order to obtain the points in Figure 2 we diluted the nematic phase until there was no more birefringence observed. We presume that this concentration is equal to the concentration of rods in isotropic phase coexisting with the nematic phase.

To interpret the data in Figure 2 we need to introduce the concept of the effective diameter ( $D_{\text{eff}}$ ). The isotropic-nematic phase transition for very long rods can be described at the level of the second virial coefficient, as was first recognized by Onsager (Onsager 1949). The prediction of the theory is that the isotropic phase becomes unstable when following condition is satisfied:  $c\pi L^2 D/4 = 4$ , where  $c$  is rod number density, while  $L$  and  $D$  are the length and the diameter of the rod. In the same paper Onsager showed how to incorporate the effect of long range repulsion due to surface charge by exchanging the bare diameter with an effective diameter  $D_{\text{eff}}$ , which can be rigorously calculated and is roughly equal to the distance between two rods where the intermolecular potential is equal to thermal energy of  $1 k_B T$ . At high ionic strength  $D_{\text{eff}}$  approaches the bare diameter, while at low ionic strength  $D_{\text{eff}}$  is much larger than the bare diameter, and is typically several Debye screening

lengths. The condition for the instability of the isotropic phase for charged rods becomes  $c \pi L^2 D_{\text{eff}}/4 = 4$ . It follows that the bare rod number density at the I-N phase transition is inversely proportional to  $D_{\text{eff}}$ . This is experimentally observed for *fd wt* over a wide range of ionic strengths as shown with square symbols in Fig. 2. The full line, which contains no adjustable parameters, is the numerical solution of the I-N transition for semiflexible rods where  $D_{\text{eff}}$  is calculated by an extension of the Onsager theory (Chen 1993).

Water at room temperature is a good solvent for PEG polymers, which approximate Gaussian coils. Thus PEG coated surfaces interact with each other through long range repulsion (Devanand & Selser 1992, Kuhl *et al.*) 1994. Therefore in our *fd*-PEG system, in addition to the already present electrostatic repulsion between the charged virus surfaces, we introduce repulsion due to the attached PEG molecules. We expect that for polymers with large molecular weight and/or at high ionic strength the dominant interparticle interaction, and consequently  $D_{\text{eff}}$  is completely determined by the polymer diameter because the ionic double layer is confined deep within the attached polymer. The opposite is true at low ionic strength and/or low molecular weight polymer. This is exactly the behavior that is shown in Figure 2. For *fd*-PEG-20,000 we observe that for ionic strengths greater than 2 mM the I - N transition is independent of ionic strength. This implies that  $D_{\text{eff}}$  for the *fd*-PEO-20,000 system is determined entirely by polymer repulsion. The effective diameter of the particle can be extracted from the I-N co-existence concentrations since we have shown that there is a relationship between the effective diameter and concentration of virus:  $c \text{ [mg/ml]} = 222/D_{\text{eff}} \text{ [nm]}$ . For *fd*-PEG-5,000 the I - N transition changes from being dominated by polymer stabilization at high ionic strength to electrostatic stabilization below 20 mM ionic strength. Because this transition from polymer dominated to electrostatic dominated repulsion occurs at a higher ionic strength for *fd*-PEG-5,000 compared to *fd*-PEO-20,000, the effective diameter of *fd*-PEG-5,000 is smaller than that for *fd*-PEO-20,000. The formula relating the molecular weight ( $M_w$ ) of PEG to its radius of gyration ( $R_g$ ) is  $R_g = 0.215 M_w^{0.583} \text{ \AA}$  (Devanand & Selser 1992). From Figure 2 we can calculate that *fd*-PEG-20000 system has  $D_{\text{eff}} = 45 \text{ nm}$ , which is approximately equal to  $D_{\text{bare}} + 4R_g = 35 \text{ nm}$ . *fd*-PEG-5000 complex has  $D_{\text{eff}} = 17 \text{ nm}$  at high ionic strength, while  $D_{\text{bare}} + 4R_g = 19 \text{ nm}$ . This suggests the model of the polymer being a sphere of radius  $R_g$  attached to the surface of the virus, although we expect that the polymer is deformed by the virus to some extent. In principle, if the exact shape of the repulsive interaction between two polymer covered cylindrical surfaces is known, and if the number of attached polymers per virus is measured, it would be possible to theoretically calculate the phase diagram for rods with attached polymers and compare it to experimental findings. However, we have not yet developed a method to accurately measure the polymer surface coverage.

We can use our system of rods with different diameters to study some basic problems in the physics of colloidal liquid crystals. To prepare a binary mixtures of rods with different diameters we simply mix *fd wt* and *fd*-PEO. The ratio of the diameters is equal to the ratio of the concentrations at which these two systems undergo the I-N transition. An additional advantage of this system is that this ratio can be altered in continuous way by simply adjusting ionic strength. From Fig. 2 it is possible to deduce that at 200 mM ionic strength the *fd*-PEO complex has effective diameter about 5 times thicker than *fd wt*. We have observed both

isotropic-isotropic and nematic-nematic demixing in binary mixtures of *fd*-PEG-20000 and *fd* wt. Comparison to available theories is currently underway (Roi & Mulder 1998, Sear & Mulder 1996). In summary, a combination of molecular engineering and post-expression chemistry has resulted in the production of gram quantities of monodisperse rods varying in length from  $0.4 - 1.4 \mu\text{m}$  and diameter 10 - 50 nm.

#### 4. Phase behavior of *fd* wt virus with non-absorbing polymer

Onsager has shown how to describe the I-N transition of hard rods with large L/D ratio using the virial expansion of free energy. The second virial expansion quantitatively describes very long and thin rods at the isotropic - nematic co-existence, but fails for highly aligned and concentrated rods. As explained in the previous section, even systems that have soft repulsion can be successfully described by the Onsager theory. The reason for this is that the lowest energy state occurs when two charged rods are perpendicular to each other. Therefore, charge reduces alignment of the rods, which in turn increases the accuracy of the virial expansion (Stroobants *et al.* 1986). In contrast, if there is attraction between rods, then perfectly parallel rods are the configuration with the lowest energy. Consequently, attractions increase the overall alignment of the rods in a nematic suspension and decrease the accuracy with which the virial expansion describes the system. It was shown that for even very slightly attractive rods the third virial coefficient is almost as large as the second one (van der Schoot & Odijk 1992). Currently there is a lack of both experiments and theories describing the I-N transition in suspensions of attractive rods and our understanding of the phase behavior of rods with attraction is rather limited.

We should note that there is a recent theory that introduces attractions to the study of the I-N transition of hard rods indirectly by considering mixtures of hard rods and polymers (Lekkerkerker & Stroobants 1994). The polymers induce an effective attraction between colloidal rods through the well known mechanism of depletion attraction (Asakura & Oosawa 1958). An advantage of this system to study the influence of attractions on hard rods is that it is possible to control both the range of attraction by varying the molecular weight of added polymer and the interaction strength by altering the polymer concentration. However, there is an important difference between a hard rod/polymer mixture and suspension of pure rods with attractive interactions because for the latter the polymer concentration is different across the coexisting phases and therefore the strengths of attraction between rods in the isotropic and nematic phases are different (Lekkerkerker *et al.* 1992).

In our experimental studies of mixtures of *fd* wt and polymers we seek polymers which do not interact with the virus. The two polymers we use for this purpose are Poly(ethylene glycol) (PEG) and Dextran. To measure the I-N phase coexistence we mix concentrated *fd* virus and Dextran (M. W. 148,000), dilute the sample with buffer until two phase co-existence is initiated, and let the sample phase separate at room temperature, which takes about two weeks for the slowest phase separating sample. The  $R_g$  of 148,000 Dextran is about 11 nm (Nordmeier 1993, Senti *et al.* 1955). In order to measure the concentration of both rods and polymers in the coexisting isotropic and nematic phases we use fluorescently labeled FITC-Dextran.

After appropriate dilution the concentrations of both polymer and *fd* is measured on the spectrophotometer. The resulting phase diagram is shown in Fig. 3. At low polymer volume fraction the coexisting I-N concentrations change little from the pure virus limit and there is little polymer partitioning between the coexisting phases. At higher polymer volume fractions the phase diagrams “opens up” and we measure the coexistence between a polymer-rich rod-poor isotropic phase and a polymer-poor highly concentrated nematic phase. The qualitative features in such a phase diagram are very similar to the theoretically predicted phase diagram (Lekkerkerker & Stroobants 1994, Bolhuis *et al.* 1997). In a forthcoming publication we will present detailed experiments of the effects of ionic strength, polymer nature, and molecular weight on the phase diagram (Dogic *et al.* 2001).

When the phase diagram “opens up”, the concentration of the rods in the nematic phase coexisting with the isotropic phase dramatically increases. For the ionic strength of 100 mM *fd* virus forms a stable smectic phase at 160 mg/ml (Dogic & Fraden 1997) so it is reasonable to expect a stable isotropic-smectic (I-S) phase coexistence to supersede the I-N transition for high enough polymer volume fraction. Indeed, experiments show that there is a stable I-S coexistence. Since the size of our virus allows us to visualize individual smectic layers with an optical microscope we can observe the nucleation and growth of the smectic phase out of an isotropic suspension in real time. Observation of typical structures and their temporal evolution are summarized in the remainder of this paper. All the following images were taken with a Nikon optical microscope using DIC optics equipped with a 60x water immersion lens and condenser.

The typical I-N tactoid that forms in the two phase region of pure hard rods, or rods with weak attractions (i. e. low polymer volume fraction) is shown in Figure 4a. The nematic phase appears as a bright droplet elongated along the nematic director with a dark background of isotropic rods. In the picture, the rods are parallel to the plane of the paper and tend to align parallel to the I-N boundary. As the polymer concentration is further increased we initially observe nematic droplets as shown in Fig. 4a, but after a few minutes the droplets begin to change their morphology. Figures 4a to 4k were all taken from the same sample and show the time evolution of an initially smooth tactoid during the first 20-30 minutes of phase separation. In Fig 4b we observe a thin helical sheet wrapped around the nematic tactoid. The width of the sheet along the direction of the tactoid is about 1  $\mu\text{m}$ . We assume that this sheet is a single smectic layer of rods parallel to the direction of the nematic tactoid that has nucleated on the nematic surface. This smectic layer continues to grow and becomes thicker as shown in the side views of the tactoid in Figs 4c and 4d. Figure 4e shows the same helical structure, but this time viewed from above (the alignment of the rods is perpendicular to the paper). We observe that the helical smectic layer can close itself to form a single ring around the nematic tactoid. A typical example of this structure is shown in Fig. 4f where the rods are pointing out of the paper, and in Fig. 4g where rods are parallel to the paper. Two striped tactoids with smectic rings can coalesce (Fig. 4h) to form droplets with a variable number of smectic rings as is shown in Fig. 4i, 4j and 4k. Figure 4k to 4m are taken at increasing volume fraction of polymers. From these three figures we observe that with increasing polymer concentration the thickness of the smectic rings increases in comparison to the size of the nematic core. The striped nematic droplets encircled with smectic layers will proceed to coalesce until they sediment to the bottom of

the sample and reach a size that is many tens of microns. It should also be noted that not all tactoids have the closed ring structures, but some instead have a helical structure that has a beginning and an end. This has important consequences for the further progress of phase separation as is demonstrated in Fig. 5.

After the sample has been phase separating for few hours we observe a new kind of structure shown in Fig. 5a. These are filaments of *fd* that have a cross section of  $1\mu\text{m}$ , which corresponds to a one particle length. The director is oriented perpendicular to the fiber axis and precesses in a helical fashion as in a cholesteric. This results in the helical structures observed in optical micrographs. The connection between the twisted sheets and the striped tactoids from Fig. 4 coexisting in the same sample is clearly shown in Fig. 5c. The twisted strands grow slowly out of the smectic rings and over a period of few days the strands are able to reach lengths of several hundred microns. We should note that the twisted strand is a metastable structure with a pronounced tendency to untwist over a period of days or as one moves along the length of the strand away from its root at the striped I-N droplet. For example Fig. 5b to 5g where all taken from the same sample and show very different degrees of twisting. Two strands can also connect with each other as is shown in Fig. 5f. The twisted strands can quite often form a helical superstructure. Figure 5e is focused onto the bottom and Fig. 5g is focused on the top of such a structure. Perhaps such a structure has its origin in a striped tactoid (Fig 5c) that has for some reason lost its nematic core.

After a few months, as the sample further evolves towards equilibrium we observe a number of large sheets that are one rod length thick. We believe that these are essentially large smectic membranes. Using the microscope we photograph a sequential series of images in the plane of focus (*xy* plane, Fig. 6a) evenly spaced at  $0.2\mu\text{m}$  intervals in the *z* dimension and from this information we reconstruct the structure of the membrane in three dimensions. Fig. 6c shows the image of the membrane perpendicular to the alignment of the rods from which we deduce that the diameter of the membrane is about  $10\mu\text{m}$ . The cuts through the *xy* and *yz* planes are uniformly one micron thick along the *y* direction.

In another series of experiments we studied a mixture of *fd* virus and PEG polymer (M. W. 35,000,  $R_g = 9.6\text{ nm}$ ) shown in Fig. 7. The concentration of rods (10 mg/ml) was lower than in the Dextran/virus mixture described previously, but the ionic strength was again 110 mM. We increased polymer concentration until we observed slight turbidity in our sample indicating the onset of two-phase coexistence. The structures we observed under these conditions with PEG/virus mixtures are very similar to the structures observed in Dextran/virus mixtures illustrated in the previous three figures. As we increased the polymer concentration further, we observed a direct formation of the smectic membrane out of isotropic suspension, instead of their growth from the striped nematic tactoid. An image of such a membrane, where all the rods point out of the surface of the paper is shown in Fig. 7a. The side view (not shown) indicates that the membrane is essentially one rod length thick. The membranes are stable over a period of hours, which is surprisingly long. If the sample is observed for long enough it is possible to observe the process of coalescence of two smectic membranes. Fig. 7e shows such a process in a sequence of frames spaced 1/30 seconds apart. In the first frame the rods in both membranes are aligned in the same direction. Once the membranes are aligned, the process of coalescence is complete in about 0.16 seconds.



As the concentration of the polymer is increased further another pathway to the formation of the smectic phase is observed. We presume that this process initially begins with the formation of the smectic membranes just as the one described in the previous paragraph. However, these membranes never reach the size of the membranes at lower polymer concentration, which coalesce sideways as is shown in Fig. 7e. Instead, while the membranes are quite small they stack on top of each other to form long filaments shown in Fig. 7c. Within a few seconds after mixing the sample these filaments form a percolating network, which is self supporting and does not sediment over time. As is seen in Figs. 7c the thickness of the filament is not uniform, but varies from one layer to the other. The irregular thickness of the filaments does not change even if the sample is left to equilibrate for few days. From this we can conclude that it takes rods a very long time to diffuse from one layer to another. We also observe that as the concentration of the polymer is increased, the thickness of the filament decreases. The formation of the filaments can be understood in terms of depletion attraction. Once a single smectic layer grows to a critical size a lower energy is achieved by stacking two equal diameter membranes on top of each other rather than by letting two membranes coalesce laterally. This is because the strength of the attraction between two surfaces is proportional to the area of the interacting surfaces.

It is well known that depletion attraction between a colloid and a wall is much stronger than the attraction between two colloids (Dinsmore *et al.* 1997; Sear 1998). Because of this, in parallel to the bulk phase transitions described previously, there are competing transitions with the surface of the container. Some of the structures we observe on the surfaces due to the depletion attraction are shown in Fig 7f and 7g. Fig. 7f shows a single smectic layer of rods. By focusing through the layer in  $z$  direction we conclude that this layer is extremely thin (upper limit of  $0.2 \mu\text{m}$ ). Furthermore, these layers can stack on top of each other as is shown in Fig. 7g.

Up to now, all the experiments were done with polymers of roughly the same radius of gyration (Dextran 150,000 has  $R_g = 11 \text{ nm}$ , PEG 35,000 has  $R_g = 9.6 \text{ nm}$ ) and at same ionic strength (110 mM). When we decrease the radius of the polymer (PEG 8,000 has  $R_g = 4.1 \text{ nm}$ ) we still observe two-dimensional membranes which are composed of parallel rods. However, as is shown in Fig. 8, the membranes assume a hexagonal shape, which strongly implies that the rods within the membrane are not a two dimensional fluid, but a two-dimensional crystal. Figures 8a to 8d were taken at the lowest polymer concentration at which the crystallization was observed. Under these conditions the induction time for critical nuclei formation as indicated by the turbidity of the sample is about 30 minutes. A typical image of a 2D crystal where the rods within the crystal are pointing out of the plane of the paper is shown in Fig. 8a, while the side view where the alignment of the rods is in the plane of the paper is shown in Fig 8b. The thermal fluctuations within the crystal are easily visible under the microscope and the crystal is easily deformed as is visible in the side view of the crystal. Often, instead of observing a flat membrane, we observe a membrane with screw dislocation located at the nucleation center. The images of such a membrane from the top view and side view are shown in Fig. 8c and 8d. In Fig 8c we can clearly see that the two layers are on top of each other, but if we focus through in the  $z$  direction we observe that these two layers belong to the same 2d crystal. This is exactly what we would expect from a crystal that has a screw dislocation.

If we increase the polymer concentration, the induction time decreases and an image of these post-critical nuclei is shown in Fig. 8e. A typical crystal that usually grows overnight out of this solution is shown in top view in Fig. 8f, while Fig. 8g shows the side view of such a crystal. A nucleation center that significantly protrudes out of the 2D crystalline membrane is clearly visible, and sometimes it is even possible to observe two 2D crystal membranes connected through the same nucleation center as shown in Fig 8h. It is important to note that such a nucleation center is visible in every 2D crystalline membrane and at all polymer concentrations. Two-dimensional crystals have been observed in rod-like TMV/BSA mixtures (Adams & Fraden 1998a) and these crystals also have a clearly visible single nucleation site protruding. The fact that the structures observed in PEG/fd and TMV/BSA system are extremely similar suggest that the features of 2D crystalline membranes summarized here are generic to any system of rods with short range attraction. At even higher polymer concentration, the induction time is unmeasurably short and typical nuclei that are formed almost instantaneously are shown in Fig. 8j. The resulting crystals display almost no thermal fluctuations, are much smaller than crystals formed at low polymer concentration, their number density is much higher, and typically their edges are much sharper and better defined as is shown in Fig. 8k and 8l.

The influence of both polymer concentration and polymer range has been extensively studied for three dimensional spherical colloids (Hagen & Frenkel 1994, Gast *et al.* 1986, Lekkerkerker *et al.* 1992). The basic parameter that determines the behavior of the system is the ratio of the range of attraction between colloids as compared to the range of the effective hard core repulsion. On the one hand, if the range of attraction is very short the vapor-liquid phase transition will be metastable with regards to the vapor-crystal transition for all conditions. On the other hand, if the range of attraction is sufficiently long ranged under certain conditions the vapor-liquid transition will supersede the vapor-crystal phase transition. Our results on the formation of two dimensional membranes in the polymer/virus mixtures agree with this general rule. In the mixture of large polymer (Dextran M. W. 150,000,  $R_g = 11$  nm) and *fd* virus the attraction is long ranged and we observe a two dimensional liquid like membrane. In contrast, in the mixture of small polymer PEG 8,000,  $R_g = 4$  nm) where the attraction is short ranged, we observe a two dimensional crystalline membrane.

## 5. Conclusions

In the first two sections of this paper have demonstrated the production of monodisperse rod-like *fd* and M13 viruses for which the contour length and effective diameter was systematically altered. We plan to use these viruses to study smectic phase formation as a function of contour length to persistence length, and the use the polymer-grafted *fd* to study smectic phase formation as a function of the range of interparticle repulsion. We also plan to study the effects of bidispersity and polydispersity in both diameter and length on the liquid crystalline phase transitions. In the latter portion of this paper, we summarized the behavior of virus/polymer mixtures, which behave as hard rods with an attractive potential. Although the interactions between rods in polymer solutions is very simple, we observe a whole range of novel structures of surprising complexity. These experiments and previous

studies on rod/sphere mixtures (Adams *et al.* 1998) indicate that there is much that remains to be understood about the phase behavior of such mixtures.

## 6. Acknowledgment

This research was supported by the NSF Grant. We thank Kirstin Purdy for preparation of the cloned virus pGT-N28. Additional information, movies, and photographs are available online at: [www.elsie.brandeis.edu](http://www.elsie.brandeis.edu)

## References

- Adams, M., Dogic, Z., S. L. Keller & S. Fraden. 1998 Entropically driven microphase transitions in mixtures of colloidal rods and spheres. *Nature* **393**, 349.
- Adams, M. & Fraden, S. 1998 Phase behavior of mixtures of rods (tobacco mosaic virus) and spheres (polyethylene oxide, bovine serum albumin). *Biophys. J.*, **74**, 669.
- Asakura, S. & Oosawa, F. 1958 Interactions between particles suspended in solutions of macromolecules. *J. Polym. Sci.*, **33**, 183.
- Bates, M. A. & Frankel, D. 1998 Influence of polydispersity on the phase behavior of colloidal liquid crystals: A monte carlo simulation study. *J. Chem. Phys.* **109**, 6193–6199.
- Bhattacharjee, S., Glucksman, M. J. & Makowski, L. 1992 Structural polymorphism correlated to surface charge in filamentous bacteriophages. *Biophys. J.* **61**, 725.
- Bohle, A. M., Holyst, R. & Vilgis, T. Polydispersity and ordered phases in solutions of rodlike macromolecules. *Phys. Rev. Lett.* **76**, 1396–1399.
- Bolhuis, P. G. & Frenkel, D. 1997 Tracing the phase boundaries of hard spherocylinders. *J. Chem. Phys.* **106**, 668–687.
- Bolhuis, P. G., Stroobants, A., Frenkel, D. & Lekkerkerker, H. N. W. 1997 Numerical study of the phase behavior of rodlike colloids with attractive interactions. *J. Chem Phys* **107**, 1551.
- Chen, Z. Y. 1993 Nematic ordering in semiflexible polymer chains. *Macromolecules* **26**, 3419.
- Cui, S. & and Chen, Z. Y. 1994 Columnar and smectic order in binary mixtures of aligned hard cylinders. *Phys. Rev. E.* **50**, 3747.
- Devanand, K. & Selser, J. C. 1991 Asymptotic behavior and long-range interactions in aqueous solutions of poly(ethylene oxide). *Macromolecules* **24**, 5943.
- Dinsmore, A. D., Warren, P. B., Poon, W. C. K. & Yodh, A. G. 1997 Fluid-solid transitions on walls in binary hard-sphere mixtures. *Europhys. Lett.* **40**, 337–342.
- Dogic, Z. & Fraden, S. 1997 The smectic phase in a colloidal suspension of semi-flexible virus particle. *Phys. Rev. Lett.* **78**, 2417.
- Dogic, Z. & Fraden, S. 2000 Cholesteric phase in virus suspensions. *Langmuir* **16**, 7820–7824.
- Dogic, Z., Adams, M. & Fraden, S. 2001 to be published.
- Fraden, S. Phase transitions in colloidal suspensions of virus particles. In *Observation, Prediction, and Simulation of Phase Transitions in Complex Fluids* (ed. Baus, M., Rull, L. F. & Ryckaert, J. P.), pp 113–164. Kluwer Academic Publishers, 1995.
- Gast, A. P., Russel, W. B. & Hall, C. K. 1986 An experimental and theoretical study of phase transitions in the polystyrene latex and hydroxyethylcellulose system. *J. Colloid Interface Sci.* **109**, 161.
- Hagen, M. H. J. & Frenkel, D. 1994 Determination of phase diagram for the hard-core attractive yukawa system. *J. Chem. Phys.* **101**, 4093–4097.

- Herrmann, R., Neugebauer, K., Pirkel, E., Zentgraf, H. & Schaller, H. 1980 Conversion of bacteriophage fd into an efficient single-stranded DNA vector system. *Molec. gen. Genet.* **177**, 231–242.
- Koda, T. & Kimura, H. 1994 Phase diagram of the nematic-smectic A transition of the binary mixture of parallel hard cylinders of different lengths. *J. Phys. Soc. Jpn.*, **63**, 984.
- Kuhl, T. L., Leckband, D. E., Lasic, D. D. & Isrealachvili, J. N. 1994 Modulation of interaction forces between bilayers exposing short-chained ethylene oxide headgroups. *Biophys. J.* **66**, 1479.
- Lekkerkerker, H. N. W., Coulon, P., der Haegen, V. & Deblieck, R. 1984 On the isotropic-nematic liquid crystal phase separation in a solution of rodlike particles of different lengths. *J. Chem. Phys.* **80**, 3427–3433.
- Lekkerkerker, H. N. W., Poon, W. C. K., Pusey, P. N., Stroobants, A. & Warren, P. B. 1992 Phase behavior of colloid + polymer mixture. *Europhys. Lett.* **20**, 559.
- Lekkerkerker, H. N. W. & Stroobants, A. 1994 Phase behaviour of rod-like colloid + flexible polymer mixtures. *Nuovo Cimento D* **16**, 949.
- Livolant, F. 1991 Ordered phases of dna in vivo and in vitro. *Physics A* **176**, 117–137.
- Maguire, J. F., McTague, J. P. & Rondalez, F. 1980 Rotational diffusion of sterically interaction rodlike macromolecules. *Phys. Rev. Lett.* **45**, 1891–1894.
- Maniatis, T., Sambrook, J. & Fritsch, E. F. 1989 *Molecular Cloning*, New York: Cold Spring Harbor University Press.
- Meyer, R. B. 1990 Ordered phases in colloidal suspensions of Tobacco Mosaic Virus. In *Dynamics and Patterns in Complex Fluids* (ed., Onuki, A. & Kawasaki, K.), pp 62. Springer-Verlag.
- Nordmeier, E. 1993 Static and dynamic light-scattering solution behavior of pullulan and dextran in comparison. *J. Phys. Chem.* **97**, 5770.
- Onsager, L. 1949 The effects of shape on the interaction of colloidal particles. *Ann. NY Acad. Sci.* **51**, 627.
- Polson, J. M. 1997 First-order nematic-smectic phase transition for hard spherocylinders in the limit of infinite aspect ratio. *Phys. Rev. E* **56**, R6260.
- Sato, T & Teramoto A. 1994, Statistical mechanical theory for liquid-crystalline polymer solutions. *Acta. Polymer.* **45**, 399–412.
- Sear, R. P. & Mulder, B. M. 1996 Phase behavior of a symmetric binary mixture of hard rods. *J. Chem. Phys.* **105**, 7727–7734.
- Sear, R. P. 1997 Depletion driven adsorption of colloidal rods onto a hard wall. *Phys. Rev. E* **57**, 1983–1989.
- Senti, F. R., Hellman, N. N., Ludwig, N. H., Babcock, G. E., Tobin, R., Glass, C. A. & Lamberts, B. L. 1995 Viscosity, sedimentation and light-scattering properties of fractions of an acid-hydrolyzed dextran. *J. Poly. Sci.*, **17** 527.
- Stroobants, A. 1992 Columnar versus smectic order in binary mixtures of hard parallel spherocylinders. *Phys. Rev. Lett.* **69**, 2388.
- Stroobants, A., Lekkerkerker, H. N. W. & Odijk, T. 1986 Effect of electrostatic interaction on the liquid crystal phase transition in solutions of rodlike polyelectrolytes. *Macromolecules* **19**, 2232.
- Tang, J. & Fraden, S. 1995 Isotropic-cholesteric phase transition in colloidal suspensions of filamentous bacteriophage fd. *Liquid Crystals* **19**, 459–467.
- Tkachenko, A. V. 1996 Nematic-smectic transition of semiflexible chains. *Phys. Rev. Lett.* **77**, 4218–4221.
- van der Schoot, P. & Odijk, T. 1992 Statistical theory and structure factor of semidilute solution of rodlike macromolecules interacting by van der Waals forces. *J. Chem. Phys.* **97**, 515–524.

- van der Schoot, P. 1996 The nematic-smectic transition in suspensions of slightly flexible hard rods. *J. Phys. II France* **6**, 1557.
- van Roij, R. & Mulder, B. 1996 Demixing versus ordering in hard rod mixture. *Phys. Rev. E* **54**, 6430.
- van Roij, R., Mulder B. & Dijkstra, M. 1998 Phase behavior of binary mixture of thick and thin hard rods. *Physics A* **261**, 374–390.
- Vroege, G. J. & Lekkerkerker, H. N. W. 1992 Phase transitions in lyotropic colloidal and polymer liquid crystals. *Repts. on Prog. Phys.*, **8**, 1241.
- Wen, X., Meyer, R. B. & Caspar, D. L. D. 1989 Observation of Smectic-A ordering in a Solution of Rigid-Rod-Like Particles. *Phys. Rev. Lett.* **63**, 2760.

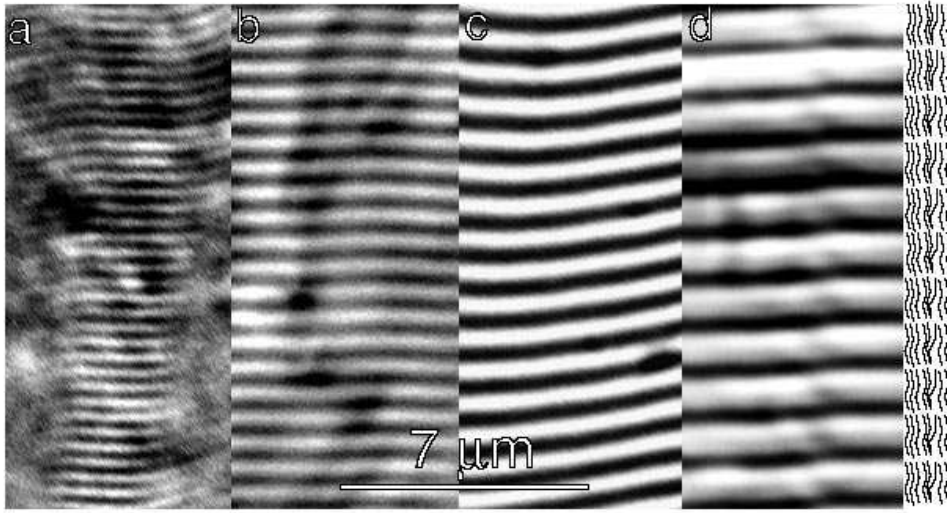


Figure 1. Optical micrographs of smectic phases of three different M13 constructs and *fd wt* (c). The periodic pattern is due to smectic layers that are composed of two dimensional liquids of essentially parallel rods, as indicated in the cartoon on the right. From left to right, the contour length of the rod-like viruses forming the smectic phase are  $0.39\ \mu\text{m}$ ,  $0.64\ \mu\text{m}$ ,  $0.88\ \mu\text{m}$ , and  $1.2\ \mu\text{m}$ . The smectic spacing measured from optical micrographs is  $0.40\ \mu\text{m}$ ,  $0.64\ \mu\text{m}$ ,  $0.9\ \mu\text{m}$  and  $1.22\ \mu\text{m}$  from image (a) to (d) respectively.

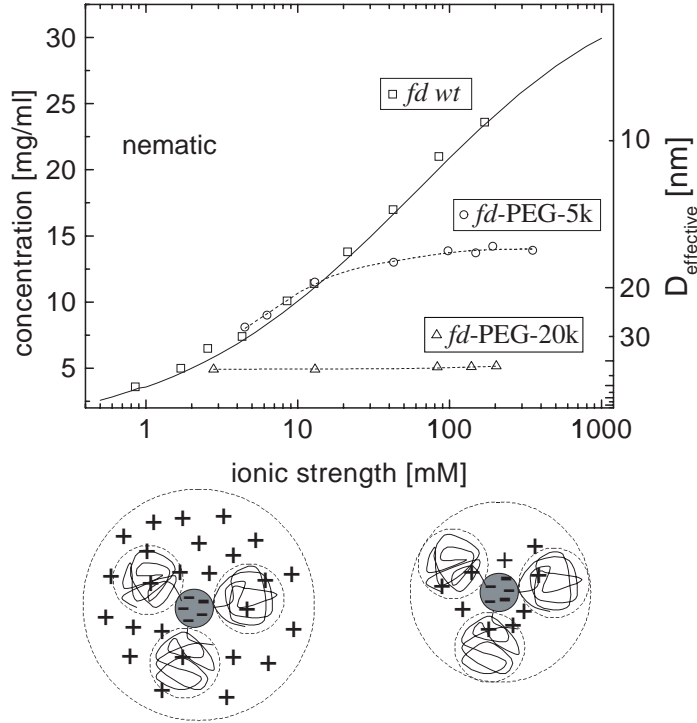


Figure 2. Concentration of the virus rods in coexisting isotropic and nematic phases as a function of ionic strength and thickness of the PEG layer covalently attached to the virus. Square points indicate the I-N transition in *fd wt* and were taken from previous work (Tang & Fraden 1995). The relationship between the I-N co-existence concentration ( $c$ ) and electrostatic effective diameter is  $c[\text{mg/ml}] = 222/D_{\text{eff}}[\text{nm}]$  and is drawn as a solid line. Circles indicate the I-N transition in *fd* coated with PEG-5,000, while triangles refer to the *fd* virus coated with PEG-20,000. When calculating the concentration of *fd*-PEG we only take into account the *fd* core since the polymer density is not known. The dashed lines are a guide for the eye. At low ionic strength, electrostatic repulsion determines  $D_{\text{eff}}$ , while the grafted polymer sets  $D_{\text{eff}}$  at high ionic strength, as indicated in the cartoon of a cross-section of the PEG-virus complex.

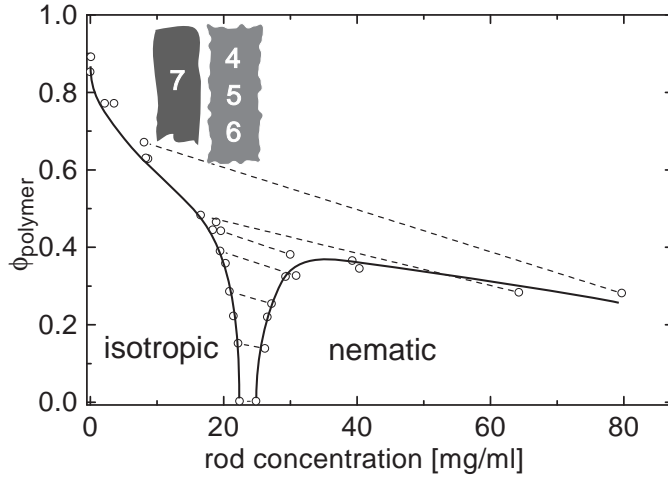


Figure 3. Phase diagram of *fd wt* and Dextran (M. W. 148,000) mixture at 200 mM ionic strength. The  $R_g$  of Dextran was taken to be 11nm and vertical axis is given by  $\phi_{\text{polymers}} = (4\pi R_g^3/3)(N/V)$  where  $N/V$  is the number density of Dextran polymers. The dashed lines are tie lines between coexisting isotropic and nematic phases. Not all of the coexistence lines are shown for clarity. The full lines are a guide to the eye indicating the boundary of the two phase region. At high polymer concentration the rods do not form a uniform phase, but a percolating network which does not completely sediment and therefore we are not able to measure its concentration. The region of the phase diagram labeled “4” corresponds to the conditions of the samples in Figure 4, although the ionic strengths are different.



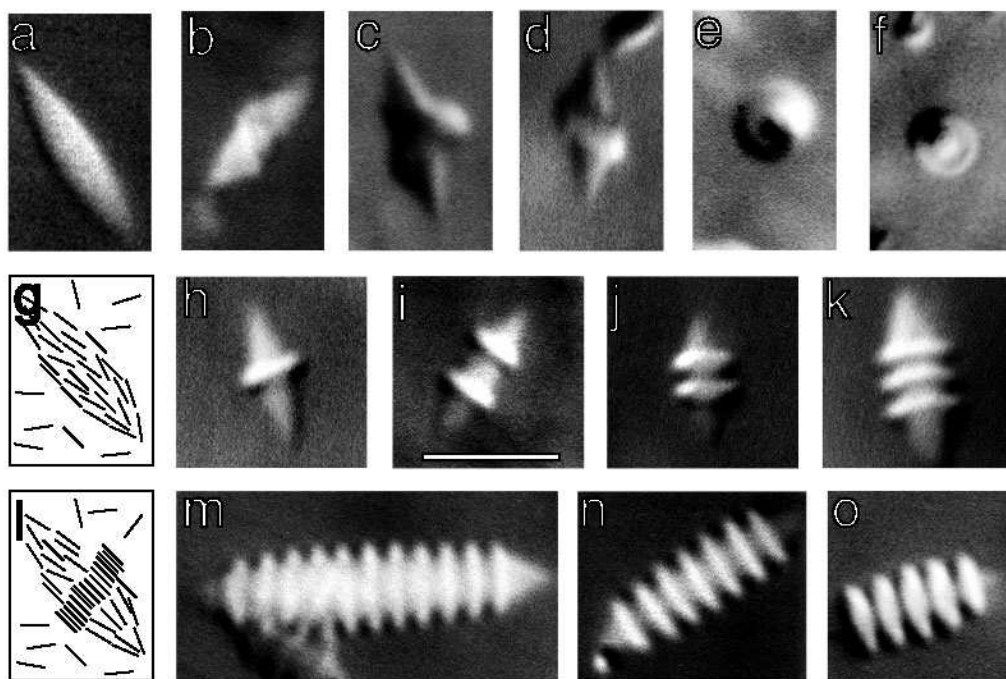


Figure 4. Initial stages of the phase separation of an initially isotropic suspension *fd* at concentration of 22 mg/ml and Dextran (M. W. 150,000) that shows the formation of striped tactoids upon addition of Dextran. The ionic strength is 110 mM. The concentration of polymer in picture (a) to (f) and (h) to (k) is constant and was added to the pure virus suspension until it became slightly turbid. The concentration of polymer increases in samples (m) to (o). In figure (g) we sketch the conformation of rods in typical tactoid at I-N transition in rods without attraction. The sketch of the nematic tactoid with the smectic ring is shown in figure 1. The scale bar is 5  $\mu\text{m}$  long and all images are taken at same magnification.

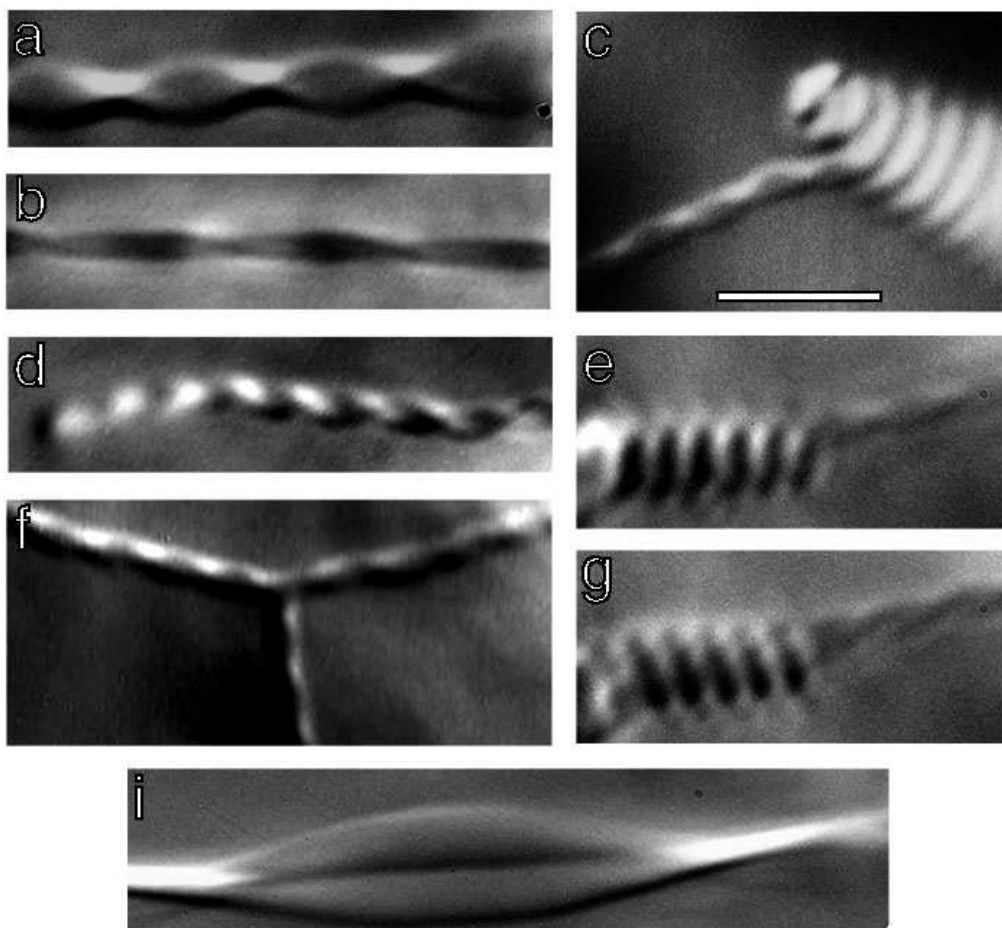


Figure 5. The twisted strands in (b) to (g) are with the same conditions as in Figure 4(a). Figure 5(a) is taken at a higher polymer volume fraction, while figure 5(i) is taken at lower virus concentration (5 mg/ml). The scale bar indicates 5  $\mu\text{m}$ .

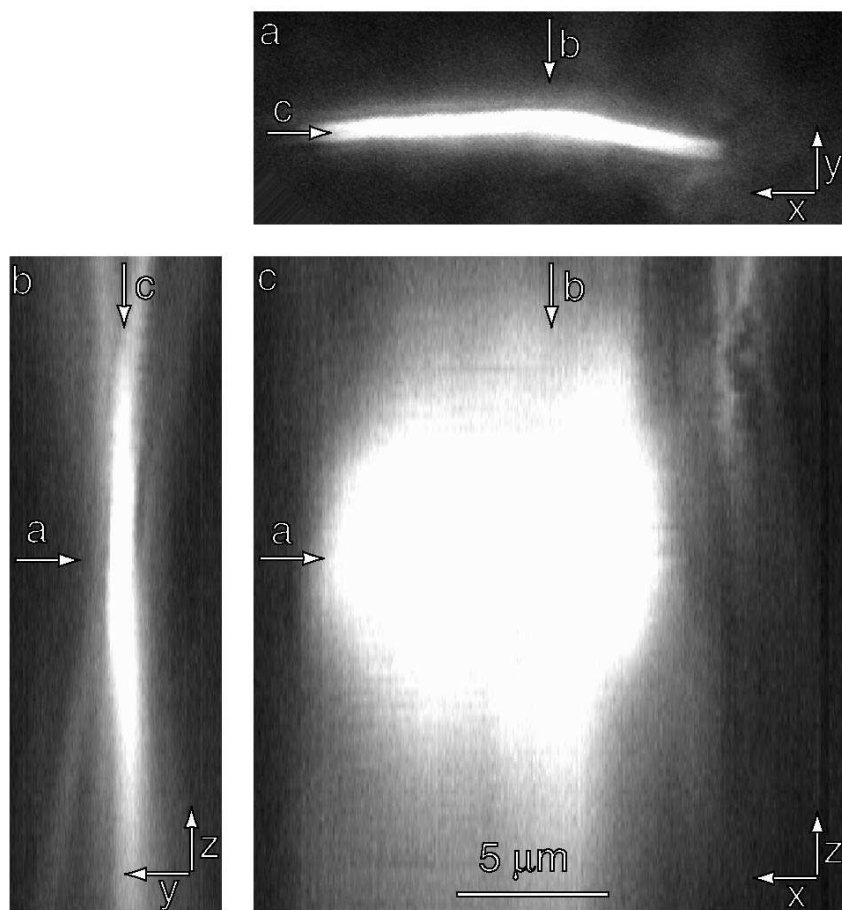


Figure 6. A three dimensional reconstruction of a large membrane of a single layer smectic that is observed in a mixture *fd wt* and Dextran 150,000 M.W. after the it has been equilibrating for 2 months. Using the microscope a sequential series of images in the  $xy$  plane at different depths  $z$  (Fig 6a) were taken and the image was reconstructed in three dimensions. Figure 6b shows the image of the membrane cut along the  $y$  direction at the position indicated by arrow (b) in figure 6(a) and 6(c). Equivalently, figure 6c shows the cut of the membrane perpendicular to the virus axis as indicated by arrow (c) in figures 6(a) and 6(b). The scale bar indicates  $5\ \mu\text{m}$ .

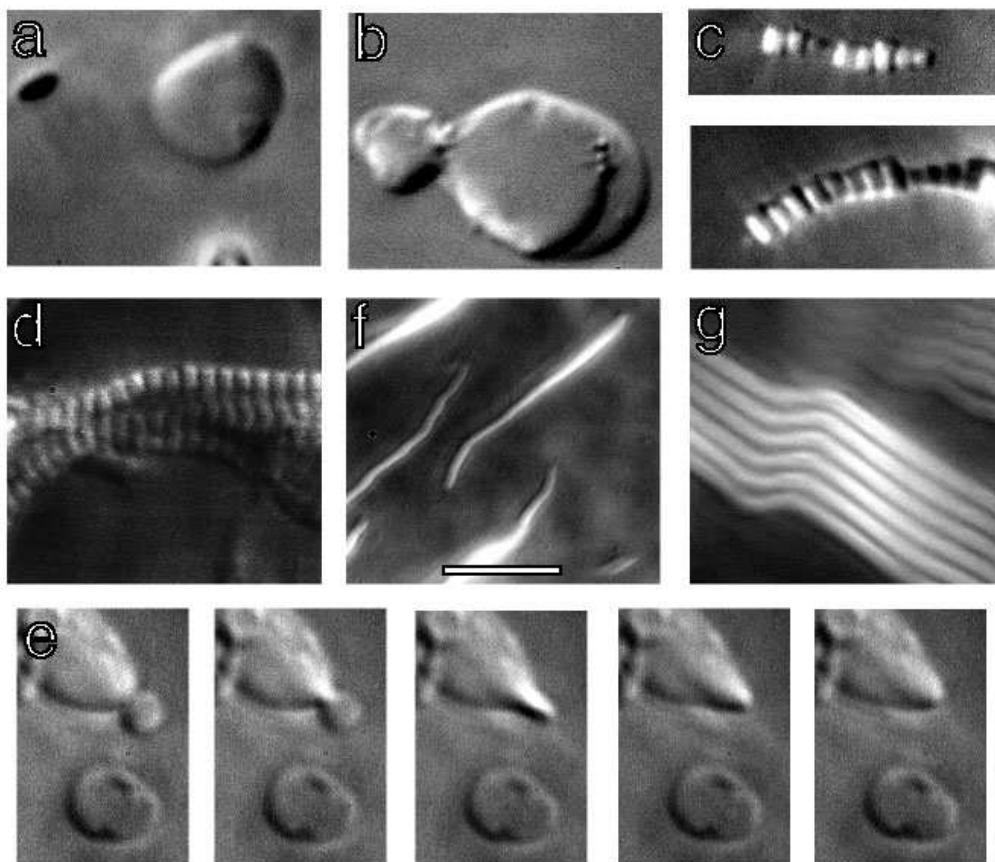


Figure 7. Phase behavior of mixture *fd* and PEG (M. W. 35,000). At the lowest concentrations of polymer we observe striped tactoids that are very similar to the ones shown in previous figures. As the concentration is increased, we observe formation of a single membrane one rod-length thick that is shown in figures 7a and 7b. In figure 7e, five successive video frames spaced 1/30 of seconds apart show coalescence of two smectic membranes. At an even higher volume fraction of polymer, we observe filaments shown in figures 7c and 7d that percolate throughout the entire sample. The phase transitions on the surface are shown in figures 7f and 7g. The scale bar indicates 5  $\mu\text{m}$ .

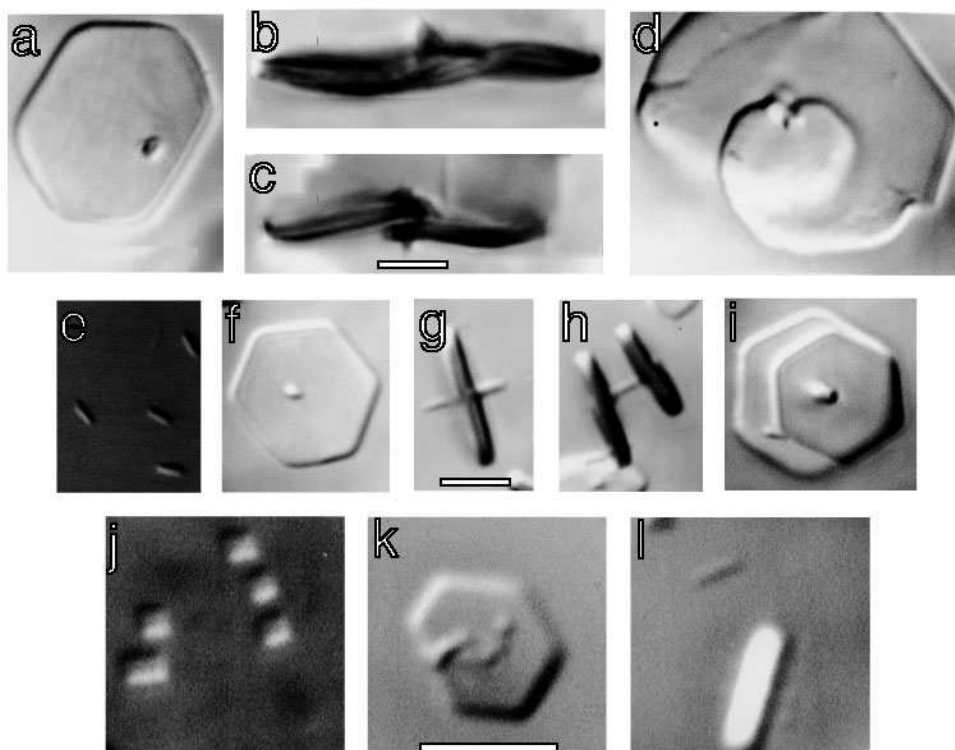


Figure 8. Optical micrographs of two dimensional virus crystals observed in mixture of PEG (M.W. 8,000) and *fd* virus at a constant concentration of 15 mg/ml. The first row of the pictures is at lowest polymer concentration at which the crystals were observed, the second row is at intermediate polymer concentration and third row is at highest polymer concentration. The scale bars are 5  $\mu\text{m}$  and images in each row are at the same magnification.